



**HAL**  
open science

# Computational chemistry approaches for the preparation of supported catalysts: progress and challenges

Manuel Corral Valero, Pascal Raybaud

## ► To cite this version:

Manuel Corral Valero, Pascal Raybaud. Computational chemistry approaches for the preparation of supported catalysts: progress and challenges. *Journal of Catalysis*, 2020, 391, pp.539-547. 10.1016/j.jcat.2020.09.006 . hal-03001978

**HAL Id: hal-03001978**

**<https://ifp.hal.science/hal-03001978>**

Submitted on 12 Nov 2020

**HAL** is a multi-disciplinary open access archive for the deposit and dissemination of scientific research documents, whether they are published or not. The documents may come from teaching and research institutions in France or abroad, or from public or private research centers.

L'archive ouverte pluridisciplinaire **HAL**, est destinée au dépôt et à la diffusion de documents scientifiques de niveau recherche, publiés ou non, émanant des établissements d'enseignement et de recherche français ou étrangers, des laboratoires publics ou privés.

# **Computational chemistry approaches for the preparation of supported catalysts: progress and challenges**

**M. Corral Valero<sup>1</sup>, P. Raybaud<sup>1,2,\*</sup>**

<sup>1</sup> IFP Energies nouvelles, Rond-point de l'échangeur de Solaize, BP 3, 69360 Solaize, France.

<sup>2</sup> Univ Lyon, ENS de Lyon, CNRS, Université Claude Bernard Lyon 1, Laboratoire de Chimie UMR 5182, F-69342 Lyon, France

**KEYWORDS:** density functional theory, catalyst preparation, catalyst activation, alumina, additives, metals, sulfides

## 1. Introduction

Michel Che pioneered the fundamental concepts of Interfacial Coordination Chemistry (ICC) applied to the “craft” of heterogeneous catalysis preparation, which remains a strategic stage for the catalyst’s life.[1] Since these earlier concepts, the atomic scale’s understanding of the genesis of a heterogeneous catalyst remains highly challenging, despite numerous relevant experimental works in this area.[2-7] Indeed, shortcomings in this scientific field come from the fact the catalyst’s genesis involves chemical reactions that take place in interfacial liquid-solid or gas-solid media, where characterization as well as molecular simulation techniques are challenged. Thus, most current preparation protocols are mainly optimized by trial and error approaches based on the experimentalist’s chemical intuition or by high throughput experimental mapping. One of the directions proposed by Michel Che in his paper published in the Proceedings of the 10<sup>th</sup> International Conference in Catalysis encouraged “to perform theoretical calculations to provide a more solid foundation to model the elementary steps describing the catalyst preparation at a molecular scale.”[1] Almost thirty years later, one must recognize that the atomic scale’s insights of computational chemistry into catalyst preparation remains scarce.

Thanks to the progress of theoretical chemistry and the historical development of density functional theory (DFT),[8, 9] many research works have been devoted either to the fine description of the active sites and mechanisms of the “working catalyst”[10] or to the identification of structure-activity relationships such as “volcano curves”, [11-13] both contributing to the rational design of heterogeneous catalysts. However, computational chemistry (including DFT based approaches) may have an equally important role to play in the rational understanding of the genesis of heterogeneous catalysts (particularly when supported) in order to provide relevant “theoretical” guides and descriptors on the optimal pathways to prepare a targeted catalyst.

In this perspective, we propose an overview on how computational chemistry recently began to pave the way in this direction and which methods may contribute even more to this challenging field in the near future. For that purpose, we will consider the relevant and generic case study of alumina-supported catalyst. Firstly, we briefly recall the main chemical steps and materials involved in heterogeneous catalysts' preparation. Then, we show and discuss the computational chemistry methods and their applications to the various steps of catalysts' preparation. We finally highlight some possible future emerging research topics.

The preparation of a supported catalyst follows a rather complex stepwise procedure involving several key steps shown in Figure 1: synthesis and thermal treatment of the alumina support starting from the boehmite precursor, impregnation of the support with metallic salts and (in)organic additives, drying/calcination and activation. Figure 1 also illustrates some examples of quantum molecular models that will be discussed in the course of this perspective. Depending on the catalyst formulation, the (in)organic additives may be added at the different stages of the preparation in order to tune the interaction of the metal with the support and to optimize its further activation.[7, 14] It is well documented that each one of these steps may have an impact on the final properties of the supported active phase (chemical state, electronic structure, size and morphology), although it is often difficult to identify the precise origin in the preparation steps on the resulting catalytic properties.

As for the impregnation procedure, incipient wet impregnation (IWI) is the most widespread method in both industry and academia. It consists on the impregnation of the catalyst support by an aqueous mother solution containing metallic salt complexes with or without (in)organic additives. The impregnated material is then dried and/or calcined and the supported metal phase is activated by either hydrogen reduction and/or sulfidation depending on the type of the targeted active phase (metals, sulfides...).

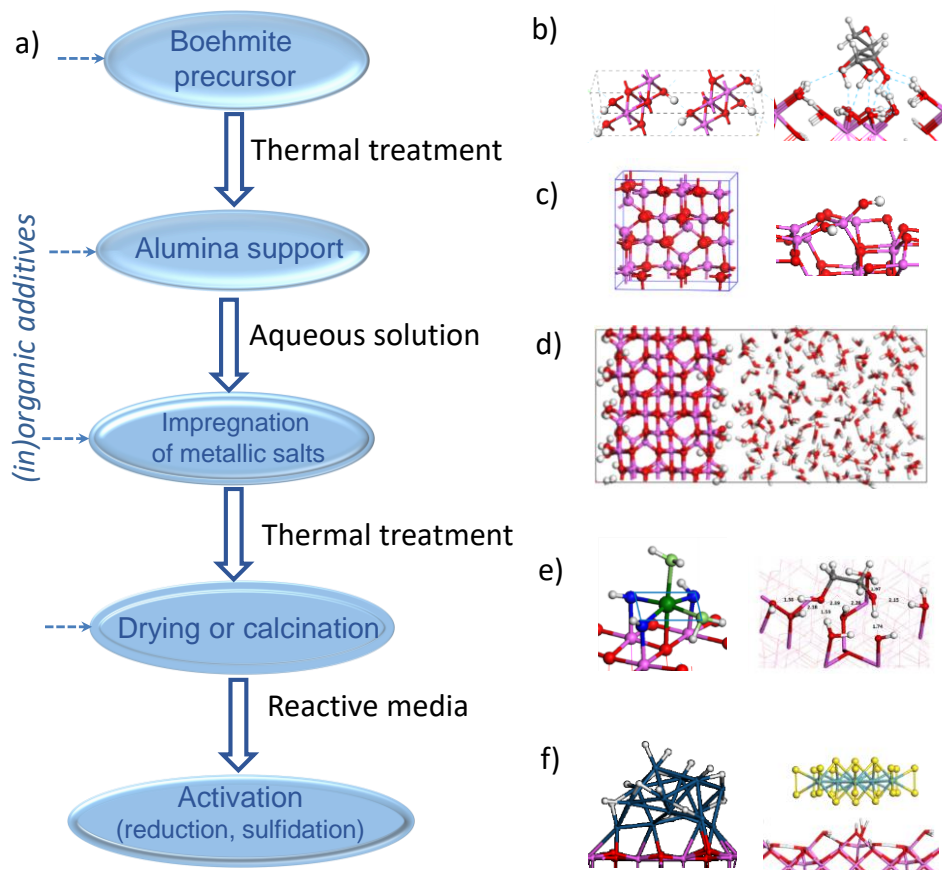


**Figure 1:** Usual synthesis pathways of heterogeneous catalysts (a) and molecular models illustrating the various stages in the case of alumina supported catalysts: b) boehmite precursors (left: bulk, right: adsorption of xylitol), c) alumina (left: bulk, right: surface), d) alumina-water interface, e) cobalt(II) and ethylene glycol adsorbed on a dried alumina surface, f)  $H_{14}\text{-Pt}_{13}$  (left) and  $\text{MoS}_2$  (right) clusters supported on alumina. The dashed arrows indicate the possible addition of organic or inorganic additives.

Each of the previous steps or each involved material (support, solvated precursors, ...) is challenging by itself. So, accounting for the combined chemical properties of each component and monitoring the dynamics of each process is hopeless. Instead, one should be inspired by Roal Hoffmann's quote: "Observables in chemistry may be the resultant of several simultaneously operative physical mechanisms... But theory has no problem in resolving

mechanisms. One can calculate contribution of each physical factor.”[15] In this way, quantum simulation may provide a set of well-quantified descriptors related to the each individual steps of the genesis of a supported catalyst:

- local architecture of the support’s anchoring/grafting sites,
- nature and strength of the metallic phase/(in)organic additives/support interaction (chemical or electrostatic bonding) during impregnation, or upon various thermal treatments (calcination, drying),
- reaction mechanisms (including transition states) involved during phase transformation (upon activation).

## 2. Methods

For addressing these questions, the robust machinery of molecular simulation can be used by combining various theoretical levels. *State of the art* DFT approaches [8, 9] provide relevant atomic scale insights on the structures and energies of the adsorption modes and transition states[16]. On top of these calculations, thermal and entropic corrections can be calculated within the formalism of ab initio thermodynamics to determine the relative stability of key intermediates as a function of (T, p) reaction conditions. Simultaneously diverse spectroscopy simulations (vibrational frequencies, core level shift, chemical shift, ...) are very useful to make the link with in situ characterizations (infrared, X-ray photoelectron spectroscopy, nuclear magnetic resonance, X-ray absorption spectroscopy...). Here, we recall that some aspects challenging the expected “chemical accuracy” of *state of the art* DFT [17] must be carefully checked before simulating the genesis of a supported catalyst in the same way as it is achieved for the simulation of the reactivity of catalysts’ surface models. As the various steps of heterogeneous catalysts (before activation) often involve transition metal (hydr)oxide precursors at interfacial systems, some questions on the accuracy of results may arise from the

difficult treatment of electron correlation (either static or dynamic) in DFT, such as self-interaction errors, multi-reference systems, and long ranged electron interaction.[18, 19] To overcome some of these problems, one has to choose properly the exchange-correlation functional (including in some cases dispersion corrections or Hartree-Fock exchange). Moreover, some of the most complex open-shell systems may even require to go beyond the Kohn-Sham DFT formalism or at least to check DFT reliability by using multi-configurational methods, which are very computationally demanding and cannot be yet systematically applied to the systems of this perspective.[19]

As we will illustrate it for the impregnation step, simulating solid-liquid interface for catalysis is rather challenging [20] and it is often required to go beyond static approaches and explore the potential energy surface by free or biased ab initio molecular dynamics (AIMD) [21, 22] which is rather computationally demanding when the solvent is treated explicitly by quantum method. For that purpose, the solvent can in some cases be treated implicitly by a continuum model parametrized by the value of its dielectric constant.[23] Alternatively, empirical force field based molecular dynamics and Monte-Carlo simulations are also very useful to address larger scale effects by generating an ensemble of configurations and determining the dynamics and equilibrium properties for complex binary systems. Nevertheless, the utilization of the latter approaches is scarce in catalysis since most catalytic reactions involve chemical bond formation and cleavage phenomena which need the development of non-standard reactive force-fields by fitting the parameters on ab initio calculations for benchmark systems.[24]

### 3. The catalyst support under thermal treatment

We will consider here the gamma polymorph of aluminum oxide ( $\gamma$ -alumina or  $\gamma$ - $\text{Al}_2\text{O}_3$ ), which is the support of many active phases used in numerous industrial catalytic processes such as hydrotreatment,[7] Fischer-Tropsch synthesis,[25] hydrocracking,[26] naphtha reforming[27], alkane dehydrogenation,[28] or biomass conversion,[29-31]. The reasons for this choice in so many applications are multiple: alumina exhibit versatile textural properties (such as tunable pore distribution, and surface areas of about  $250 \text{ m}^2 \text{ g}^{-1}$ ) as well as local surface structures with tunable acid-basic properties useful for impregnation and reactivity.  $\gamma$ - $\text{Al}_2\text{O}_3$  and other polymorphs are usually prepared from the calcination of aluminum mono- ( $\text{AlOOH}$ ) or tri-hydroxides ( $\text{AlO}(\text{OH})_3$ ) such as boehmite (Figure 1b left), gibbsite, tohdite, diaspore or bayerite.[32] Calcination of any of these hydroxides at temperatures above  $1000 \text{ }^\circ\text{C}$  leads to the formation of  $\alpha$ - $\text{Al}_2\text{O}_3$  (corundum). Metastable forms of  $\text{Al}_2\text{O}_3$  can be obtained by quenching the calcination procedure at lower temperatures. The  $\gamma$ -alumina form is the outcome of boehmite calcination at  $450 \text{ }^\circ\text{C}$ . Since the bulk structures of these hydroxides are well defined, it was possible to show how the relative thermodynamic stability and the transition temperatures of bulk mono- and tri-hydroxides can be recovered by combining DFT calculations with a thermodynamic model of the dehydration process.[33] However, in order to go beyond in the field of catalyst synthesis, we need to understand the behavior of nano-crystallites of such hydroxydes and  $\gamma$ -alumina itself. During the thermal treatment, the synthesis of  $\gamma$ -alumina involves the topotatic transformation of boehmite,[34] that is, the morphology of  $\gamma$ -alumina nano-crystallites is inherited from the one of the boehmite precursor. This transformation impacts the textural properties of alumina supports, namely surface area and pore volume, as they can be either the outcome of complex agglomeration phenomena either of alumina nano-crystallites during calcination or of boehmite nano-crystallites in solution prior to its calcination into alumina.

Interestingly, it was possible to capture by DFT simulation the essence of the boehmite to  $\gamma$ -alumina bulk dehydration process.[35] In particular, AIMD simulations reveals first the inter-layer mobility of protons leading to water formation inside the structure of boehmite activated at rising temperature. Then, geometry optimization shows how the water release induces a collapse of the boehmite structure through a cross linking of adjacent layers and shearing movement. Last but not least, the Al atoms migrate from their initial positions, in an octahedral coordination environment, to other positions in which they bind to the oxygen sublattice in tetrahedral coordination centers following a pairwise diffusion. One should bear in mind that this atomistic model is not based on the spinel  $\text{MgAl}_2\text{O}_4$  structure though some local features around Al centers are recovered. Firstly, the plot of the thermodynamic profile along this complex process leads to the identification of relevant bulk structures for  $\gamma$ -alumina where the distribution of Al atoms is more complex than the defective spinel like structure of  $\text{MgAl}_2\text{O}_4$  usually evoked for this solid [34], since Al occupies non spinel sites in octahedral and tetrahedral positions with vacancies in both octahedral and tetrahedral spinel sites (Figure 1c left). The occupation of non-spinel sites was also confirmed by other DFT calculations [36] combined to extensive computational screening of  $\sim 1.5$  billion structural candidates and force-field energy minimization of 122000 structures.[37]

Beyond this bulk model, slab models allowed to solve the nature and concentration of the surface OH groups on the most abundant facets (110), (100) and (111) exposed by alumina crystallites as a function of thermal treatment and water vapor pressure within ab initio thermodynamic formalism.[38-40] This model enabled to revisit the experimental IR spectra of the hydroxyl groups present at the surface in gas phase (Figure 1c right),[41] but also Al NMR experiments.[42] Besides, surface energies of the support were evaluated and compared to micro-calorimetry measurements:[43] these are key descriptors to predict equilibrium morphologies of alumina crystallites [44], morphology effects on materials acid-basic

properties, and how sintering effects might occur under thermal treatment. Following an earlier proposal made by Busca,[45] the most recent extension of these molecular models including the edges of the alumina crystallites enables to rationalize the  $^1\text{H}$  NMR spectra of the hydroxyls groups of the support.[46]

This analysis has proven to be one important step forward in the rationalization of the chemical properties of this support as, during the preparation of a catalyst, the precursors anchor predominantly with the hydroxo groups at the surface,[1] as we will illustrate in what follows.

## **4. The catalyst support in water solution**

### **4.1 The boehmite precursor**

Due to particularities of the calcination process of boehmite into alumina, that is, the effects driven by the so-called topotactical transformation, it is critical for the support's synthesis to understand how the boehmite precursor may influence the resulting alumina agglomeration and its textural properties. This can be controlled by selective modification of the surface energies of the different exposed boehmite facets in aqueous solution. However, simulating solid-aqueous solution at variable pH is not feasible nowadays by the sole use of DFT simulation. One reasonable compromise is to evaluate DFT surface energies and structures at the pH corresponding to the Zero Point of Charge (ZPC) and to compute the surface energy change as the surface charge evolves with the protonation and deprotonation of the various OH modeled at the DFT level. The latter requires knowledge of the hydroxo groups' protonation constants (pKa) which can be obtained with reasonable accuracy from the empirical multi-site complexation model (MUSIC) [47-49] or more complex AIMD simulations such as those in ref.[50]. In the latter example, AIMD approach remains strongly time consuming: several millions of CPU hours on high performance computers for several

tens of picoseconds trajectories to reach the required convergence level. Once pKa constants are known, they can be used to compute surface charge as a function of pH, temperature and ionic force with software packages solving speciation in solution such as PHREEQC.[51] This approach was applied for boehmite by AIMD simulation in water [52] in order to compute the interfacial energies of this solid (001), (010) and (101) facets and determine the various OH sites present at ZPC. According to the afore-mentioned topotactic transformation, these facets will give rise to the (100), (110), (111) facets of  $\gamma$ -alumina which explains why controlling the boehmite morphology is crucial for the final support. Then, by applying the MUSIC model, the interfacial energies and Gibbs-Curie-Wulff morphology of boehmite nanocrystallites have been deduced as a function of the surrounding water pH.[53] We will illustrate this approach further in the case of alumina.

Other ways to control particle morphology involve the addition of organic additives in solution or the use of different solvents acting as selective surfactants. The impact of xylitol on boehmite morphology was investigated by a combined experimental and theoretical study.[54] In that case, it was rather efficient to use implicit solvent approach, such as the “Conductor-like Screening Model” (COSMO) [55, 56], to compute the adsorption energies of xylitol on different boehmite facets and deduce the morphology of boehmite crystallites in the presence of xylitol.[54] This organic molecule preferentially adsorbs in the hydroxyl nests of the (001) and (101) surfaces (Figure 1b right), which are thus stabilized as observed experimentally. However, the final form of the observed boehmite particles is not always driven by thermodynamics: kinetic limitations of nucleation and growth phenomena need also to be considered. In a recent work, some groups have been trying to deduce the extent at which these are affecting particle morphology (see Kerisit et al.[57], where they used a similar approach to the one of Ref.[53] in deriving, for different pH, the morphology at both thermodynamic equilibrium and kinetic limited conditions). For a full description of the

dynamics of this process, one needs to take into account the interactions between facets of finite size particles and with solution, which is beyond the possibilities of the standard periodic DFT calculations quoted above. Thus, the development of coarse-grained models to study the dynamics of nucleation and growth in solution could be a most interesting perspective in this area.

## **4.2 Impregnation of alumina**

Coming back to  $\gamma$ -Al<sub>2</sub>O<sub>3</sub> surfaces, in order to address questions related to the impregnation step, it is mandatory to simulate phenomena taking place at the solid liquid interface (SLI), to make the bridge with interfacial coordination concepts[1] and rationalize the impregnation steps. As illustrated in the case of boehmite, this remains a rather challenging question for molecular simulations in general as one needs to handle the various intricate factors involved during the impregnation step (pH, concentration of the precursors with counter-ions...). As underlined in introduction, it is recommended to proceed by a deconvolution of each chemical factor.

Some of these factors relies on the atomic scale's description of the water-alumina interface. As mentioned for boehmite, one way is to undertake AIMD of interfacial systems which requires quite large simulation cells and time to recover relevant insights such as the structure of the alumina-water interface (Figure 1d) and spectroscopic features of interfacial OH groups in water. Interestingly, the analysis of radial distribution functions show that mono-coordinated  $\mu_1$ -OH of the (110) surface are H-bond donors to water molecules (leading also to proton transfer through Grotthuss-like mechanism), whereas mono-coordinated  $\mu_1$ -OH of the (100) surface interact preferentially between themselves via an intra-surface hydrogen bond network.[58] The distinct behavior of the two surfaces in water may impact their respective reactivity with metallic precursors or additives during impregnation, which will certainly be the topic of future investigations. The structural differences between the two interfaces can be

evidenced by the simulation of their vibrational spectra (Figure 2a) showing that water induces a more pronounced red-shift of the vibrational frequencies of OH groups on the alumina (110) surface than on the (100). Such simulation should be in principle compared to experimental Attenuated Total Reflectance Infrared (ATR-IR) spectroscopy, which can be conducted on  $\gamma$ -alumina powders.[59, 60] However, one must stress that a direct experimental interpretation is challenging to achieve since the  $\gamma$ -alumina crystallites present in such powder samples do not exhibit usually one or two well-defined surfaces only but a much broader distribution of facets and edges. Nevertheless, the use of DFT simulation helps to identify precisely which site on which facet is at the origin of the observed phenomena. Alternatively, it is also proposed to work on  $\alpha$ -alumina single crystals exposing one unique well-defined surface[61] in order to identify the nature of interfacial OH groups by combining Sum Frequency Generation (SFG) spectroscopy[62] and DFT simulations[63]. Other AIMD simulations also revealed the long range effect (up to 10 Å) of the (110) surface on the water structuration and proton redistribution at the interface.[64] These effects are suspected to impact the reactivity of the interface with respect to the sorption of metallic precursors or (in)organic additives.

As for boehmite, following an AIMD analysis of the surface OH groups, the protonation constants of these hydroxo groups were computed by using the MUSIC empirical model,[48] and the surface charge of alumina powders in solution modeled with PHREEQC [51] in reasonable good agreement with experimental titration curves. This work showed that the extent at which alumina powders accumulate charge in solution depends mostly on the reactivity of mono-coordinated  $\mu_1$ -OH groups.

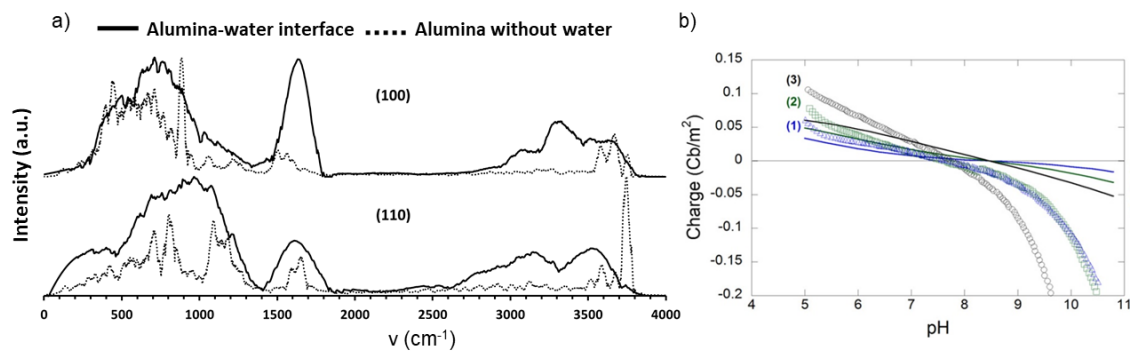


**Figure 2:** a) Calculated IR spectra for alumina OH groups of both faces in vacuum (dots) and Solid-Water Interface (line) and (b) Surface charge curves at different ionic strengths (1) 1, (2) 10, and (3) 100 mM from experiments (dots) and simulations (line). (Reprinted from reference [48], Copyright (2019), American Chemical Society)

Future works in this area should aim at computing the complexation constants between these surface groups and molecules from the impregnating solutions. This will undoubtedly make catalyst impregnation more predictable, though it is a very ambitious goal from the computational point of view.

Hence, to explore the reactivity of various species at the interface where the aqueous solvent is treated explicitly, it is mandatory to go beyond standard AIMD approaches by using biased AIMD simulations within the formalism of metadynamics[21] or blue moon sampling[22, 65] which enables the scan of the energy landscape of a given reaction. They belong to the so-called biased or constrained AIMD simulation family because the searched reaction pathway is more efficiently explored, within the limits of CPU limitations, by constraining the system along relevant collective variables (bond distances, angles, coordination number...). In addition, metadynamics simulations use a set of mathematical tools that allow the system to overcome more easily activation barriers and hence a more efficient use of computational

resources in reactivity focused studies. The latter methods have recently shown the selective interaction of polyols with specific Al surface sites of alumina in solution, which may play a role in the stabilization of alumina in hot water.[66]

An alternative approach can be provided by reactive force fields which reduce significantly the computational cost of molecular dynamics -and thus increase the number of explored configurations- for larger systems.[24] The main peculiarity of the latter approach is its ability to model bond breaking and forming mechanisms. Still, as in conventional force fields, they require, as a preliminary step, a robust parametrization of the force field against quantum calculations on benchmark systems to ensure the transferability of the force fields to a wider range of possible reactions. To further accelerate the molecular dynamics simulation, it is envisaged that machine learning approaches could also be used in close conjunction with DFT approaches to develop force fields in the course of the AIMD simulation itself.[67]

## **5. The dried/calcined catalyst**

As described in Figure 1, the next important stage of the catalyst preparation is the drying or calcination of the impregnated support. This stage features the strength and nature of interactions of the metal oxide precursor and/or (in)organic additives with the support. This will directly impact how the metal oxide precursor will be subsequently activated in reducing or sulfiding environment. This stage can be studied by *state of the art* ab initio thermodynamics and spectroscopic simulations in gas phase. The surface state of the support must be considered with great care, according to the (T, P) conditions applied during this thermal treatment (drying ~ 120°C, calcination ~ 450-500°C) which strongly influences the hydroxylation state of alumina (or any other oxides) and thus, the nature of the interaction between the precursor and the support.

The effect of residual alkaline counter-ions used in the mother impregnation solutions or in the alumina synthesis method was studied by DFT approaches and revealed how sodium cations exchange preferentially the proton of tri-coordinated  $\mu_3$ -OH leading to a  $\text{Na}^+$  species solvated by the neighboring surface OH groups and thus decreasing the surface Brønsted acidity of the support as highlighted by IR spectra and frequency calculations of the OH stretching bands.[68] Conversely, exchanging chloride anions with mono-coordinated  $\mu_1$ -OH groups was shown to enhance the surface Brønsted acidity which can be profitable for some industrial processes such as naphtha reforming.[46, 69] Interestingly, the most recent results combining  $^1\text{H}$  NMR experiments and DFT calculations indicate that chlorides preferentially exchange  $\mu_1$ -OH located at edges of the nano-crystallites.[46] Moreover, the effect of chlorides is not restricted to the support, as it may also coordinate to the metal directly as found for  $\text{Cu}^{2+}$  in an oxychlorination catalyst in reference [70], where it was reported by DFT calculations that the number of  $\text{Cl}^-$  anions bound to  $\text{Cu}^{2+}$  depends on the alumina surface and on the thermal treatment. Such a “ligand effect” of Cl atoms was also reported to stabilize Pt clusters in a highly dispersed state on alumina,[71] and is reminiscent of the earlier Che’s ICC concept.[1]

Regarding Co containing catalysts (Fischer-Tropsch and hydrotreatment), DFT calculations highlighted the most favourable anchoring sites and modes for  $\text{Co}^{2+}$  hydrated ions on the  $\gamma$ - $\text{Al}_2\text{O}_3$  surfaces following a molecular recognition mechanism comparable to an epitaxy relationship (Figure 3), [72] in the spirit of earlier proposals.[73] Such a strong metal-support interaction (involving O of the alumina network) enhances the formation of interfacial  $\text{Co}(\text{OH})_2$  phase as suggested by earlier experiments[74] which may be detrimental to the subsequent activation of Co. Similar precipitation phenomenon of  $\text{Ni}(\text{OH})_2$  has been observed by XAS also in the case  $\text{Ni}^{2+}$  on  $\alpha$ -alumina surface.[75] To avoid this, the alumina surface must be modified by silicic acid impregnation followed by a thermal treatment in order to

generate an amorphous silica-alumina layer. In this case, DFT calculations showed that the molecular recognition mechanism is strongly diminished.[72]

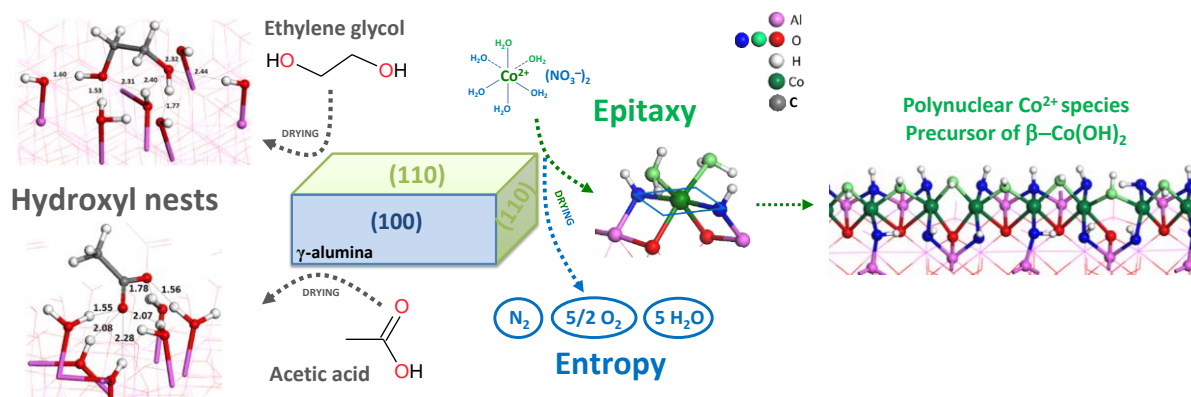


**Figure 3.** DFT optimized structures for adsorbed organic molecules (ethylene glycol and acetic acid) and  $\text{Co}^{2+}$  on alumina after drying. In the  $\text{Co}^{2+}$  containing structure, three types of O atoms are represented: O from alumina hydroxyls (blue), O from water in the Co sphere (green), O from the alumina network (red). Left part is reprinted from [76] Copyright (2018), American Chemical Society. Right part is adapted from [72].

Alternatively, organic additives are widely used nowadays in catalysis preparation to control the interaction of precursors of the metal active phase with the support as well as to optimize its subsequent activation.[7, 14] DFT calculations may identify the adsorption modes and energies of these various species under drying or calcined conditions. For acetic acid and ethylene glycols, it was shown that their interaction involve a hydrogen bond network formed between the hydroxylated alumina surface and the molecules (Figure 3).[76] As already discussed for boehmite, surface hydroxyls nests stabilizes these organic additives in some specific sites of the alumina surface, which is consistent with FT-IR characterization.[60] DFT results showed that those sites may be the same as the ones identified for cobalt for some molecules and alumina orientations, which reveals that a competition for adsorption may take

place. However, since the calculated adsorption free energies are favored for cobalt(II) due to entropic gain resulting from nitrate decomposition, it also opens the question for future works to explore the nature of the cobalt precursor used and the sequence in which cobalt and additive are impregnated.

## **6. Activation step**

This last step is a very critical one for the formation of the wished active phase and it is still the subject of numerous challenging questions, particularly when the optimal active phase must be composed of several metallic elements such as alloyed nanoparticles or mixed transition metal sulfides (TMS) nanoparticles.[77] The complexity of this step is due to the numerous chemical events involved during the reduction or sulfo-reduction steps of the oxidic precursors into the metallic or sulfided phase, respectively. Here, DFT calculations will certainly provide more relevant insights in the future in order to improve the understanding of (sulfo)reduction mechanisms in presence of  $H_2$  and/or  $H_2S$  leading to the removal of O atoms from the coordination sphere of the metals in oxide precursors. Many fundamental key questions can be addressed regarding the rate limiting steps and intermediates of the reduction, the nature and location of the most refractory O sites (on the metal or at the metal-support interface ?) In the case of the activation of  $MoS_2$  catalysts, experimental works proposed that its formation goes through a series of oxysulfides and also  $MoS_3$  intermediates, whose structures are poorly known due to their amorphous features.[78, 79] Interestingly, reverse Monte-Carlo simulations have been used to establish the first atomistic models of  $MoS_3$  exhibiting a distorted Mo chain.[80] Figure 4 illustrates ongoing DFT simulations addressing this challenging problem of the nature of supported oxysulfides and various  $MoS_3$  polymorphs before their transformation into the  $MoS_2$  active phase.[81] Significant progress

can be expected in this area in the coming years which will certainly allow to identify more systematically thermodynamic and kinetic parameters of phase transformation as a function of activation conditions. If so, this will provide the basis for in situ/operando modelling of the activation step as it has been initiated so far for catalytic reactivity.[82]

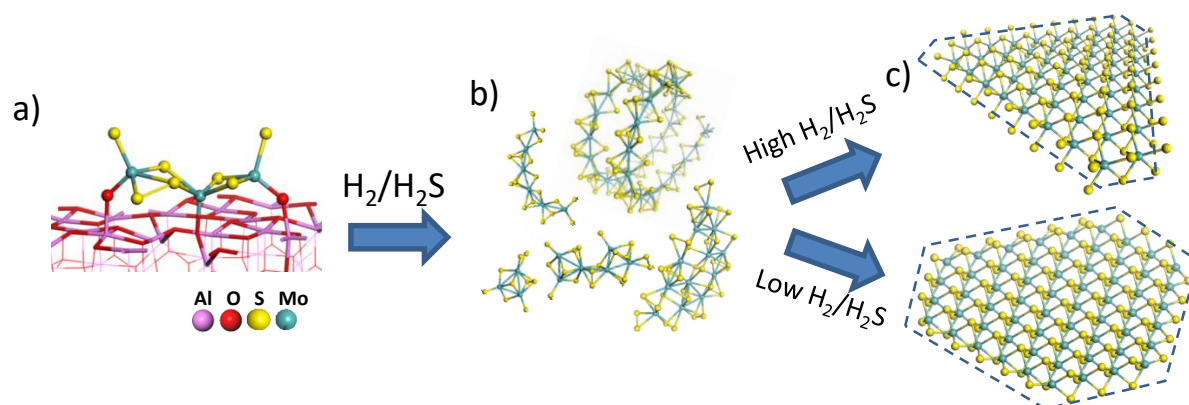


**Figure 4.** DFT structures of a) MoO<sub>x</sub>S<sub>y</sub> intermediates supported on alumina surface, and b) various MoS<sub>3</sub> polymorphs [81] suspected to be formed during the sulfidation of Mo-oxides into MoS<sub>2</sub> layers (c) with triangular or hexagonal shapes depending on H<sub>2</sub>/H<sub>2</sub>S pressures.

At this stage, ab initio thermodynamics showed how the sulfo-reductive conditions, T and  $p(\text{H}_2\text{S})/(\text{H}_2)$ , used during the activation step may impact key features of the MoS<sub>2</sub> or WS<sub>2</sub> based active phases. It was shown that the equilibrium 2D-morphology of the Mo(W)S<sub>2</sub> nanoparticles may be tuned by the H<sub>2</sub>S/H<sub>2</sub> partial pressures (Figure 4c) and several experiments have confirmed these predictions,[83-87] although we cannot exclude that 2D-morphologies can also be determined by kinetic effects induced by the precursors, the preparation methods[86] and/or support effects.[88] Moreover, ab initio thermodynamics revealed how sulfo-reductive conditions (including those used in activation conditions) impact the edge energies and thus the stability of Co and Ni promoters[89] and other first row transition

metals[90] located at the edges of Mo(W)S<sub>2</sub> phases. This shows how ab initio thermodynamics is a necessary piece of the puzzle of the so-called “in situ/operando model”.

Many key questions concern the nucleation and growth mechanisms of metallic particles from isolated atoms to clusters and to bigger particles and how they might impact the dispersion of the active phase. This requires to quantify the stability of such entities (in their oxidized and reduced state) but also their mobility on a given support which is also possible through DFT calculations. For Pd, it was shown by DFT calculations that the stability of isolated metallic atoms and diffusion rates depend strongly on the hydroxylation state of alumina:[91, 92] the stronger adsorption energies and lower diffusion rates of the isolated Pd found on the hydroxylated (110) surface than on the dehydrated (100) is interpreted to be a strong indication that the dispersion is greater on the (110) surface. For Pt<sub>1</sub>O<sub>x</sub> species (as found in some Pt oxide precursors), DFT calculations combined to HR-TEM experiments showed that the transformation of Pt<sub>1</sub>O<sub>x</sub> into large Pt oxide particles is thermodynamically unfavored with respect to their transformation into hydride Pt<sub>13</sub> cluster (Figure 1f left) in the presence of H<sub>2</sub>. [93] This underlines the role of the reduction step on the metallic particle growth mechanism. Further ab initio thermodynamics studies showed how the reduction conditions, T and p(H<sub>2</sub>), impact the resulting morphologies of Pt<sub>13</sub> cluster on alumina, [94] which has been successfully compared to in situ XANES characterization. [95]

Here again, the role of the “ligand effect” of the support on the metal can be crucial for the stabilization of highly dispersed particles with various shapes. [96] A DFT study quantified how chlorine atoms present on alumina stabilize small Pt<sub>3</sub> clusters: this effect of chlorine on particle size is actually used to maintain a high dispersion of Pt particle during the regeneration of naphtha reforming catalysts. [71] For MoS<sub>2</sub> based catalyst, an epitaxy relationship was highlighted by ab initio thermodynamics between the edges of MoS<sub>2</sub> clusters

(containing 6 Mo atoms) and anatase-TiO<sub>2</sub> surfaces which is at the origin of the higher active phase dispersion reported on the TiO<sub>2</sub> support.[88]

Once sufficient DFT data on the reaction barriers and energies of the various transformation and diffusion processes involved will be determined, kinetic Monte-Carlo approaches may be implemented to quantify the full genesis pathways as it was proposed for zeolite synthesis. [97]

## **7. Conclusions**

In this perspective, we have highlighted one of the most challenging topics for computational chemistry, related to the molecular scale description of the preparation and activation steps of heterogeneous catalysts. Although the goal to simulate the entire complexity of these steps might appear too ambitious for such theoretical approaches, we have highlighted several possible methodologies that could address some individual parts of the problem within a reductionist formalism allowing to describe correctly the chemical phenomena we want to address. We recall them here: state-of-the-art DFT, ab initio molecular dynamics (including biased AIMD), kinetic Monte-Carlo, reactive force-field molecular dynamics. We have also illustrated an example of multi-scale approach combining empirical MUSIC model and DFT descriptor to include pH effect during impregnation. Once more progress will be achieved allowing the determination of an extended database of chemical descriptors for one of the preparation steps described before, it will be possible to develop a more complete multi-scale approach taking into account preparation conditions with multi-parameters (T, pH, concentration, pressure) as it starts to be accessible nowadays for gas phase catalytic reactions.[98]

For sake of clarity, we mainly focused on alumina supported catalysts and illustrate how it is important to use a well-defined models of the support that also take into account the system

hydroxylation state at the relevant thermal and water pressure conditions of each preparation step: this plays a key role for simulating properly the phenomena involved in the so-called interfacial coordination chemistry (ICC) concepts. The computational approaches presented here can certainly be extended to other metal oxide supports and catalytic materials (as mentioned for TiO<sub>2</sub> and zeolithe synthesis above), provided that a reliable DFT model of the exposed surfaces is available.

In practice, these simulations will need larger and larger computational resources (particularly AIMD) as well as a lot of human effort in order to explore the numerous configurations and reaction coordinates involved (combination of bond distances, angles, ...) not necessarily known *a priori*. Advances in this field will go hand in hand with the novel application of mathematical techniques, some of them based in artificial intelligence methods,[99] to accelerate the sampling of multi-dimensional potential energy surfaces but also by the incentive from an ever more rational understanding of the complex chemical phenomena involved in the preparation steps of heterogeneous catalysts.

Before closing this perspective, we would like to underline that in spite of the expected continuous progress of computational methods presented before, it would be too optimistic to expect that they would fully replace experimental approaches. This is even more true than in the case of the prediction of catalytic reactivity mentioned in introduction. First, the availability of well-defined set of experimental data is highly recommended to improve and validate not yet mature simulation methodologies. Once validated, these methodologies will accelerate the research in a subsequent step, by reducing the number of “trials and errors” attempts. Finally, decoding the complex molecular phenomena involved in catalyst’s preparation should work hand in hand with experimental approaches, in order to reinforce the synergy between “in vivo” and “in silico” designed catalyst, as suggested by Michel Che three decades ago.[1]

## Acknowledgements

P.R. and M.C.V are indebted to Professor Michel Che, who was an active member of IFP New Energy Scientific Council, and shared with us his deep knowledge of catalyst preparation.

## Fundings

This work is part of the “RatiOnAl Design for CATalysis” (ROAD4CAT) industrial chair, project IDEXLYON funded by the French National Research Agency (ANR-16-IDEX-0005) and the Commissariat-General for Investment (CGI) within the framework of Investissements d’Avenir program (“Investment for the future”). Part of this work was also supported by the French National Research Agency within the framework of the ANR-14-CE08-0019 SLIMCAT project.

## REFERENCES

- [1] M. Che, *Stud. Surf. Sci. Catal.*, 75 (1993) 31-68.
- [2] K. Bourikas, C. Kordulis, A. Lycourghiotis, *Catal. Rev.*, 48 (2006) 363–444.
- [3] E. Marceau, X. Carrier, M. Che, O. Clause, C. Marcilly, *Ion Exchange and Impregnation*, in: *Handbook of Heterogeneous Catalysis*, Wiley-VCH Verlag GmbH & Co. KGaA, 2008.
- [4] P. Munnik, P.E. de Jongh, K.P. de Jong, *Chem. Rev.*, 115 (2015) 6687-6718.
- [5] K. Bourikas, C. Kordulis, A. Lycourghiotis, *Catal. Rev.*, 48 (2006) 363-444.
- [6] J.R. Regalbuto, *Catalyst Preparation: Science and Engineering*, CRC Press, USA, 2007.
- [7] H. Toulhoat, P. Raybaud, *Catalysis by Transition Metal Sulfides. From molecular theory to industrial applications.*, Technip Edition, Paris (France), 2013.
- [8] P. Hohenberg, W. Kohn, *Phys. Rev. B*, 136 (1964) 864.
- [9] W. Kohn, L.J. Sham, *Phys. Rev. A*, 140 (1964) 864.
- [10] C. Chizallet, P. Raybaud, *Catal. Sci. Technol.*, 4 (2014) 2797-2813.
- [11] J.K. Norskov, T. Bligaard, J. Rossmeisl, C.H. Christensen, *Nature Chem.*, 1 (2009) 37-46.
- [12] H. Toulhoat, P. Raybaud, *J. Catal.*, 216 (2003) 63-72.
- [13] H. Toulhoat, P. Raybaud, *Catal. Sci. Technol.*, 10 (2020) 2069-2081.
- [14] N. Koizumi, T. Mochizuki, M. Yamada, *Catal. Today*, 141 (2009) 34-42.
- [15] R. Hoffmann, *Chemical Engineering News*, (1994) 32-34.
- [16] G. Henkelman, H. Jonsson, *J. Chem. Phys.*, 113 (2000) 9978-9985.
- [17] J.P. Perdew, K. Schmidt, *AIP Conf. Proc.*, 577 (2001) 1-20.
- [18] H.S. Yu, S.L. Li, D.G. Truhlar, *J. Chem. Phys.*, 145 (2016) 130901.
- [19] C.A. Gaggioli, S.J. Stoneburner, C.J. Cramer, L. Gagliardi, *ACS Catal.*, 9 (2019) 8481-8502.

- [20] M. Saleheen, A. Heyden, *ACS Catal.*, 8 (2018) 2188-2194.
- [21] A. Barducci, G. Bussi, M. Parrinello, *Phys. Rev. Lett.*, 100 (2008) 020603.
- [22] E.A. Carter, G. Ciccotti, J.T. Hynes, R. Kapral, *Chem. Phys. Lett.*, 156 (1989) 472-477.
- [23] J. Tomasi, M. Persico, *Chem. Rev.*, 94 (1994) 2027-2094.
- [24] S. Monti, A.C.T. van Duin, S.-Y. Kim, V. Barone, *J. Phys. Chem. C*, 116 (2012) 5141-5150.
- [25] J.L. Casci, C.M. Lok, M.D. Shannon, *Catal. Today*, 145 (2009) 38-44.
- [26] C. Marcilly, *Acido-basic catalysis*, Technip Edition, Paris (France), 2005.
- [27] J.H. Sinfelt, *Handbook of Heterogeneous Catalysis*, Wiley, Weinheim, 1997.
- [28] J. Sattler, J. Ruiz-Martinez, E. Santillan-Jimenez, B.M. Weckhuysen, *Chem. Rev.*, 114 (2014) 10613-10653.
- [29] M.W. Hahn, J.R. Copeland, A.H. van Pelt, C. Sievers, *Chemsuschem*, 6 (2013) 2304-2315.
- [30] K. Larmier, C. Chizallet, N. Cadran, S. Maury, J. Abboud, A.F. Lamic-Humblot, E. Marceau, H. Lauron-Pernot, *ACS Catal.*, 5 (2015) 4423-4437.
- [31] G.W. Huber, J.N. Chheda, C.J. Barrett, J.A. Dumesic, *Science*, 308 (2005) 1446-1450.
- [32] P. Euzen, P. Raybaud, X. Krokidis, H. Toulhoat, J.-L.L. Loarer, J.-P. Jolivet, C. Froidefond, *Handbook of Porous Solids*, Wiley-VCH Verlag GmbH, Weinheim, 2002.
- [33] M. Digne, P. Sautet, P. Raybaud, H. Toulhoat, E. Artacho, *J. Phys. Chem. B*, 106 (2002) 5155-5162.
- [34] B.C. Lippens, J.H.d. Boer, *Acta Crystallogr.*, 17 (1964) 1312.
- [35] X. Krokidis, P. Raybaud, A.E. Gobichon, B. Rebours, P. Euzen, H. Toulhoat, *J. Phys. Chem. B*, 105 (2001) 5121-5130.
- [36] C. Wolverton, K.C. Haas, *Phys. Rev. B*, 63 (2001) 024102.
- [37] G. Paglia, A.L. Rohl, C.E. Buckley, J.D. Gale, *Phys. Rev. B*, 71 (2005) 224115.
- [38] M. Digne, P. Sautet, P. Raybaud, P. Euzen, H. Toulhoat, *J. Catal.*, 211 (2002) 1-5.
- [39] M. Digne, P. Sautet, P. Raybaud, P. Euzen, H. Toulhoat, *J. Catal.*, 226 (2004) 54-68.
- [40] C. Arrouvel, M. Digne, M. Breyse, H. Toulhoat, P. Raybaud, *J. Catal.*, 222 (2004) 152-166.
- [41] H. Knözinger, P. Ratnasamy, *Catal. Rev. Sci. Eng.*, 17 (1978) 31.
- [42] R. Wischert, P. Florian, C. Copéret, D. Massiot, P. Sautet, *J. Phys. Chem. C*, 118 (2014) 15292-15299.
- [43] R.H.R. Castro, D.V. Quach, *J. Phys. Chem. C*, 116 (2012) 24726-24733.
- [44] C. Arrouvel, M. Breyse, H. Toulhoat, P. Raybaud, *J. Catal.*, 232 (2005) 161.
- [45] G. Busca, *Catal. Today*, 226 (2014) 2-13.
- [46] A.T.F. Batista, D. Wisser, T. Pigeon, D. Gajan, F. Diehl, M. Rivallan, L. Catita, A.S. Gay, A. Lesage, C. Chizallet, P. Raybaud, *J. Catal.*, 378 (2019) 140-143.
- [47] T. Hiemstra, J.C.M. De Wit, W.H. Van Riemsdijk, *J. Colloid Interface Sci.*, 133 (1989) 105-117.
- [48] M. Corral Valero, B. Prelot, G. Lefevre, *Langmuir*, 35 (2019) 12986-12992.
- [49] X. Hao, W.A. Spieker, J.R. Regalbuto, *J. Colloid Interface Sci.*, 267 (2003) 259-264.
- [50] M.P. Gageot, M. Sprik, M. Sulpizi, *J. Phys.: Condens. Matter*, 24 (2012) 124106.
- [51] A.C. Parkhurst D. L., *User's guide to PHREEQC (version 2)— A computer program for speciation, batch-reaction, one-dimensional transport, and inverse geochemical calculations*, Water-Resources Investigations USGS., (1999).
- [52] P. Raybaud, M. Digne, R. Iftimie, W. Wellens, P. Euzen, H. Toulhoat, *J. Catal.*, 201 (2001) 236-246.
- [53] J.P. Jolivet, C. Froidefond, A. Pottier, C. Chaneac, S. Cassaignon, E. Tronc, P. Euzen, *J. Mater. Chem.*, 14 (2004) 3281-3288.

- [54] D. Chiche, C. Chizallet, O. Durupthy, C. Channeac, R. Revel, P. Raybaud, J.P. Jolivet, *Phys. Chem. Chem. Phys.*, 11 (2009) 11310-11323.
- [55] A. Klamt, G. Schüürmann, *Journal of the Chemical Society, Perkin Transactions 2*, (1993) 799-805.
- [56] K. Baldrige, A. Klamt, *J. Chem. Phys.*, 106 (1997) 6622-6633.
- [57] M.P. Prange, X. Zhang, M.E. Bowden, Z. Shen, E.S. Iltou, S.N. Kerisit, *J. Phys. Chem. C*, 122 (2018) 10400-10412.
- [58] B.F. Ngouana-Wakou, P. Cornette, M.C. Valero, D. Costa, P. Raybaud, *J. Phys. Chem. C*, 121 (2017) 10351-10363.
- [59] A. Davantès, C. Schlaup, X. Carrier, M. Rivallan, G. Lefèvre, *J. Phys. Chem. C*, 121 (2017) 21461-21471.
- [60] J.R. Copeland, X.R. Shi, D.S. Sholl, C. Sievers, *Langmuir*, 29 (2012) 581-593.
- [61] C. Bara, E. Devers, M. Digne, A.-F. Lamic-Humblot, G.D. Pirngruber, X. Carrier, *ChemCatChem*, 7 (2015) 3422-3440.
- [62] A. Tuladhar, S.M. Piontek, E. Borguet, *J. Phys. Chem. C*, 121 (2017) 5168-5177.
- [63] M. Sulpizi, M. Salanne, M. Sprik, M.P. Gaigeot, *J. Phys. Chem. Lett.*, 4 (2013) 83-87.
- [64] R. Réocreux, T. Jiang, M. Iannuzzi, C. Michel, P. Sautet, *ACS Applied Nano Materials*, 1 (2018) 191-199.
- [65] J. Rey, P. Raybaud, C. Chizallet, T. Bučko, *ACS Catal.*, 9 (2019) 9813-9828.
- [66] R. Reocreux, E. Girel, P. Clabaut, A. Tuel, M. Besson, A. Chaumonnot, A. Cabiac, P. Sautet, C. Michel, *Nature Communications*, 10 (2019) 1-8.
- [67] R. Jinnouchi, F. Karsai, G. Kresse, *Phys. Rev. B*, 100 (2019) 014105.
- [68] M. Digne, P. Raybaud, P. Sautet, D. Guillaume, H. Toulhoat, *Phys. Chem. Chem. Phys.*, 9 (2007) 2577-2582.
- [69] M. Digne, P. Raybaud, P. Sautet, D. Guillaume, H. Toulhoat, *J. Am. Chem. Soc.*, 130 (2008) 11030-11039.
- [70] M.J. Louwse, G. Rothenberg, *ACS Catal.*, 3 (2013) 1545-1554.
- [71] C. Mager-Maury, C. Chizallet, P. Sautet, P. Raybaud, *ACS Catal.*, 2 (2012) 1346-1357.
- [72] K. Larmier, C. Chizallet, P. Raybaud, *Angew. Chem. Int. Ed.*, 54 (2015) 6824-6827.
- [73] S. Boujday, J.-F. Lambert, M. Che, *J. Phys. Chem. B*, 107 (2003) 651-654.
- [74] S.N. Towle, J.R. Bargar, G.E. Brown, G.A. Parks, *J. Colloid Interface Sci.*, 187 (1997) 62-82.
- [75] A. Tougeriti, I. Llorens, F. D'Acapito, E. Fonda, J.L. Hazemann, Y. Joly, D. Thiaudière, M. Che, X. Carrier, *Angew. Chem. Int. Ed.*, 51 (2012) 7697-7701.
- [76] B.F. Ngouana Wakou, M. Corral Valero, P. Raybaud, *J. Phys. Chem. C*, 122 (2018) 19560-19574.
- [77] H. Topsøe, B.S. Clausen, R. Candia, C. Wivel, S. Mørup, *J. Catal.*, 68 (1981) 433-452.
- [78] E. Payen, S. Kasztelan, S. Housseny, R. Szymansky, J. Grimblot, *J. Phys. Chem.*, 93 (1989) 6501.
- [79] D. Nicosia, R. Prins, *J. Catal.*, 231 (2005) 259-268.
- [80] S.J. Hibble, G.B. Wood, *J. Am. Chem. Soc.*, 126 (2004) 959-965.
- [81] A. Sahu, S.N. Steinmann, P. Raybaud, submitted, (2020).
- [82] L. Grajciar, C.J. Heard, A.A. Bondarenko, M.V. Polynski, J. Meeprasert, E.A. Pidko, P. Nachtigall, *Chem. Soc. Rev.*, 47 (2018) 8307-8348.
- [83] H. Schweiger, P. Raybaud, H. Toulhoat, *J. Catal.*, 212 (2002) 33-38.
- [84] H. Schweiger, P. Raybaud, G. Kresse, H. Toulhoat, *J. Catal.*, 207 (2002) 76-87.
- [85] B. Baubet, M. Girleanu, A.-S. Gay, A.-L. Taleb, M. Moreaud, F. Wahl, V. Delattre, E. Devers, A. Hugon, O. Ersen, P. Afanasiev, P. Raybaud, *ACS Catal.*, 6 (2016) 1081-1092.
- [86] T. Alphazan, A. Bonduelle-Skrzypczak, C. Legens, A.S. Gay, Z. Boudene, M. Girleanu, O. Ersen, C. Coperet, P. Raybaud, *ACS Catal.*, 4 (2014) 4320-4331.

- [87] J.V. Lauritsen, M.V. Bollinger, E. Lægsgaard, K.W. Jacobsen, J.K. Nørskov, B.S. Clausen, H. Topsøe, F. Besenbacher, *J. Catal.*, 221 (2004) 510-522.
- [88] C. Arrouvel, M. Breysse, H. Toulhoat, P. Raybaud, *J. Catal.*, 232 (2005) 161-178.
- [89] E. Krebs, B. Silvi, P. Raybaud, *Catal. Today*, 130 (2008) 160-169.
- [90] R. Arancon, M. Saab, A. Morvan, A. Bonduelle-Skrzypczak, A.-L. Taleb, A.-S. Gay, C. Legens, O. Ersen, K. Searles, V. Mougél, A. Fedorov, C. Copéret, P. Raybaud, *J. Phys. Chem. C*, 123 (2019) 24659-24669.
- [91] M.C. Valero, P. Raybaud, P. Sautet, *Phys. Rev. B*, 75 (2007).
- [92] M.C. Valero, P. Raybaud, P. Sautet, *J. Phys. Chem. B*, 110 (2006) 1759.
- [93] C. Dessal, A. Sangnier, C. Chizallet, C. Dujardin, F. Morfin, J.-L. Rousset, M. Aouine, M. Bugnet, P. Afanasiev, L. Piccolo, *Nanoscale*, 11 (2019) 6897-6904.
- [94] C. Mager-Maury, G. Bonnard, C. Chizallet, P. Sautet, P. Raybaud, *Chemcatchem*, 3 (2011) 200-207.
- [95] A. Gorczyca, V. Moizan, C. Chizallet, O. Proux, W. Del Net, E. Lahera, J.-L. Hazemann, P. Raybaud, Y. Joly, *Angew. Chem. Int. Ed.*, 53 (2014) 12426-12429.
- [96] C.H. Hu, C. Chizallet, C. Mager-Maury, M. Corral-Valero, P. Sautet, H. Toulhoat, P. Raybaud, *J. Catal.*, 274 (2010) 99-110.
- [97] M. Ciantar, C. Mellot-Draznieks, C. Nieto-Draghi, *J. Phys. Chem. C*, 119 (2015) 28871-28884.
- [98] S. Matera, M. Maestri, A. Cuoci, K. Reuter, *ACS Catal.*, 4 (2014) 4081-4092.
- [99] M. Ceriotti, *J. Chem. Phys.*, 150 (2019) 150901.